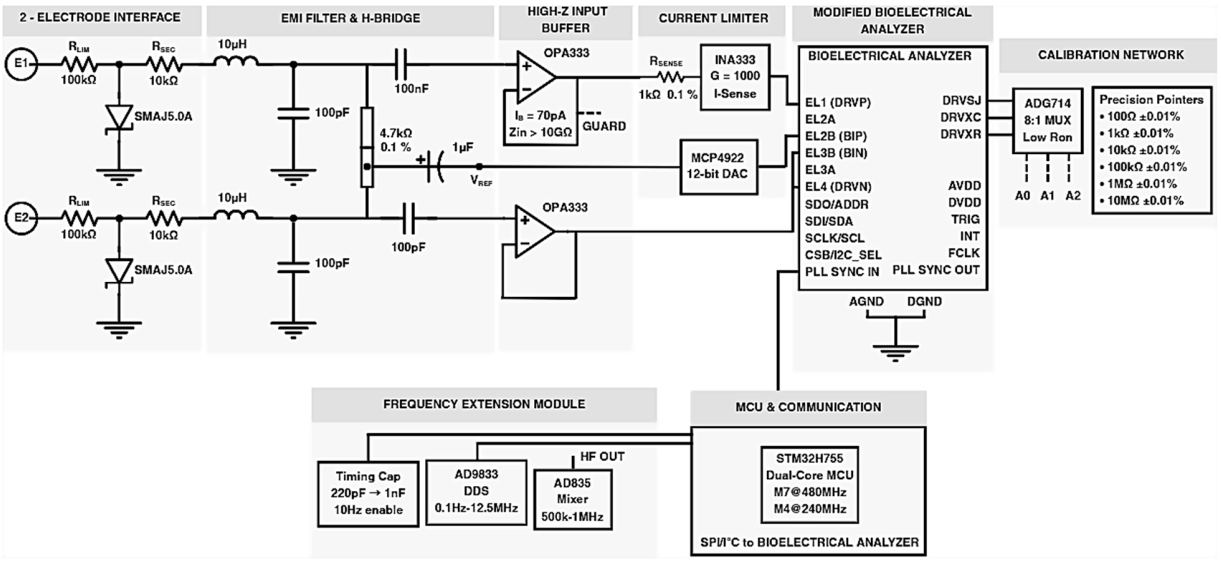


Figure S1. Bipolar (2-electrode) configuration circuit implementation for bioelectrical spectroscopy.

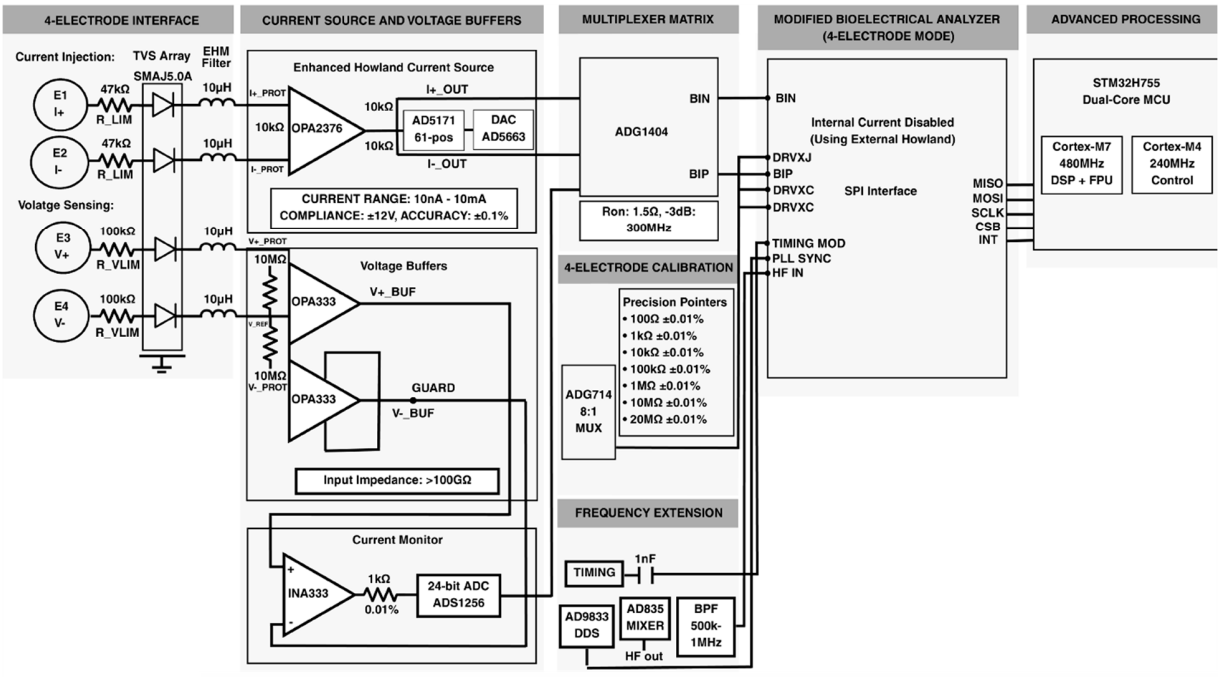


Figure S2. Tetrapolar (4-electrode) configuration circuit implementation for bioelectrical spectroscopy.

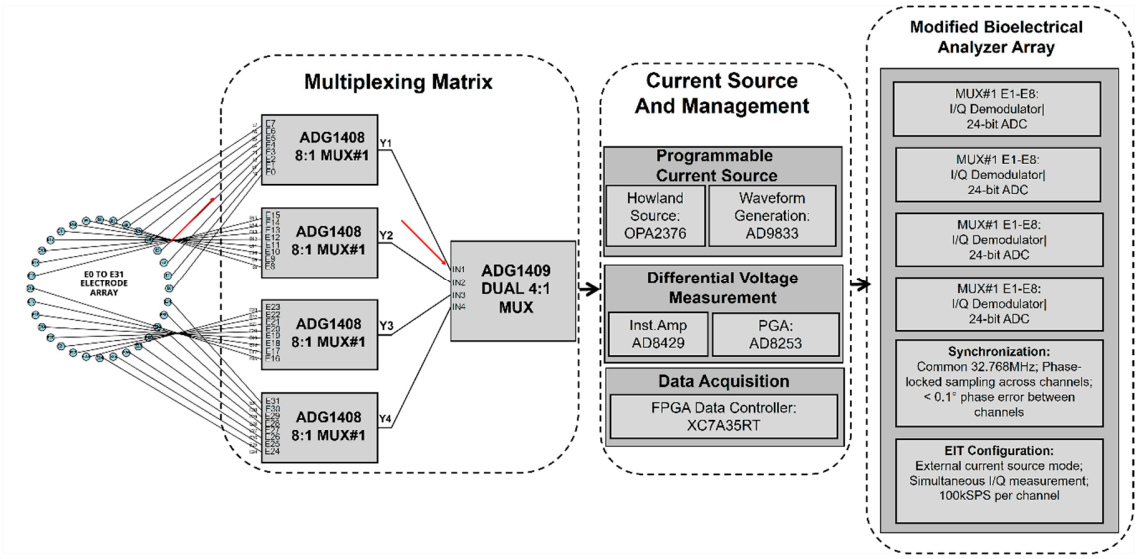


Figure S3. 32-electrode array configuration with multi-stage multiplexing architecture for tomographic applications.

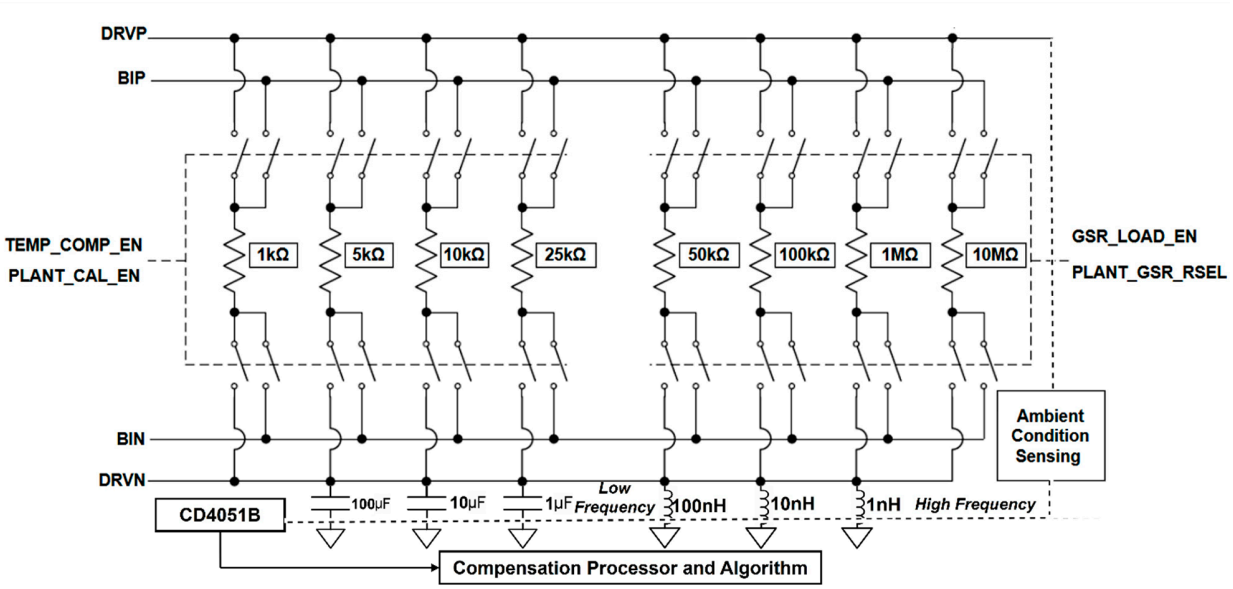


Figure S4. Precision programmable resistor load network for bioelectrical sensor system calibration.

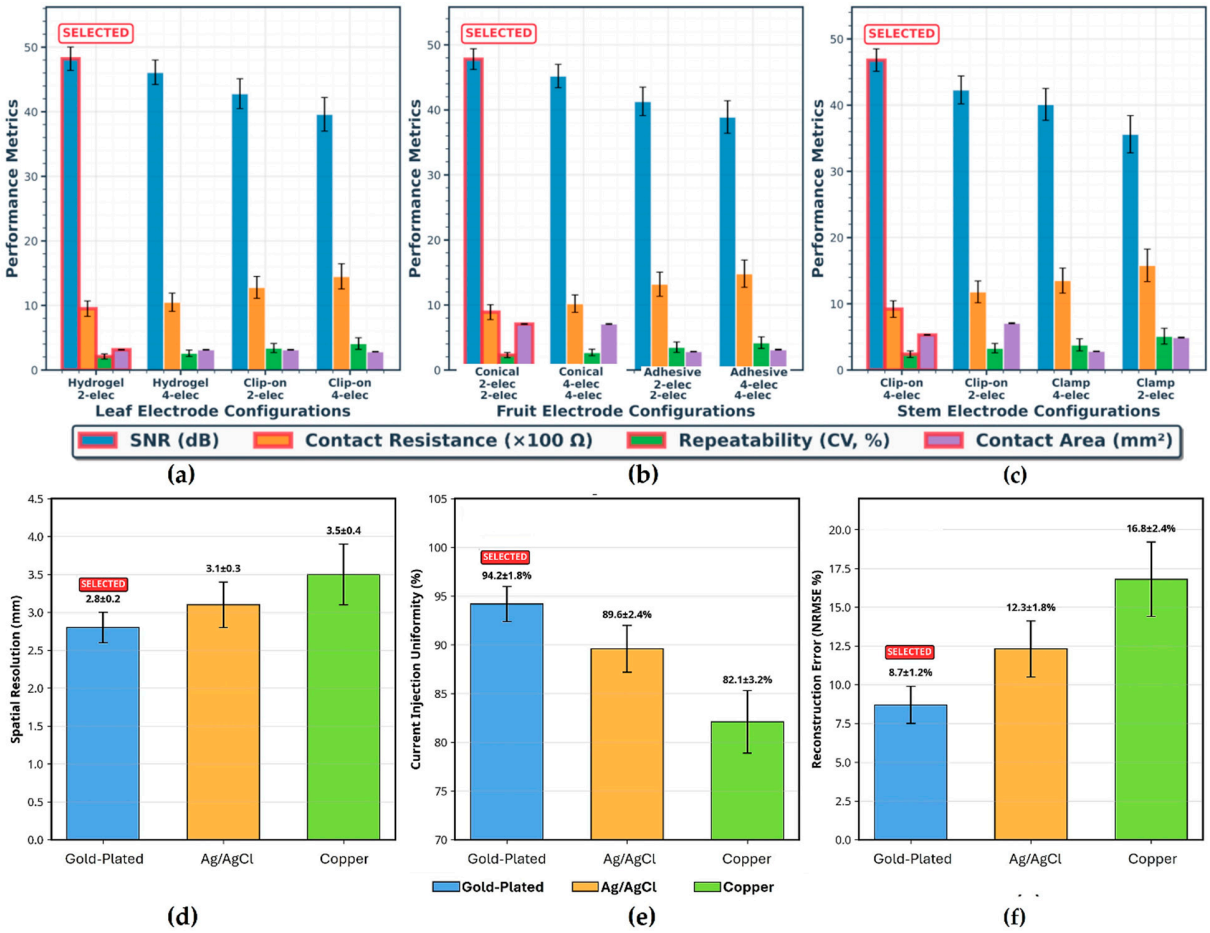


Figure S5. Electrode performance evaluation for bioelectrical spectroscopy (a-c) and tomography (d-f) measurements across strawberry plant organs.

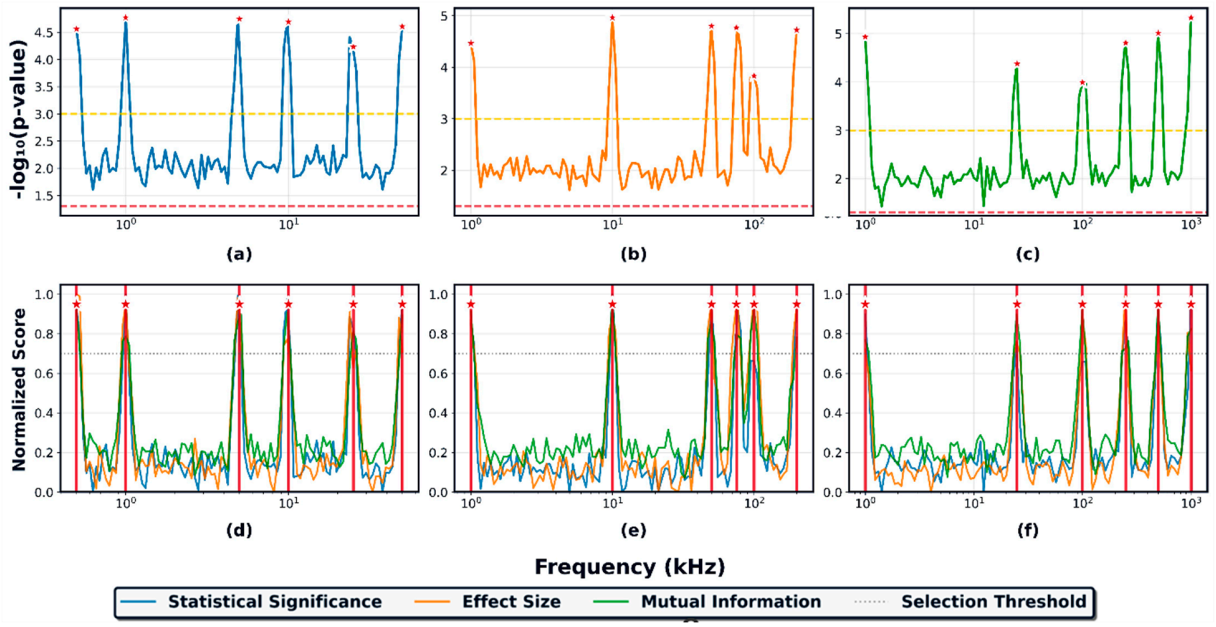


Figure S6. Statistical validation and multi-criteria frequency selection showing (a-c) -$\log_{10}$(p-values) from t-tests and (d-f) normalized scores integrating statistical significance, effect size, and mutual information for leaves, fruits, and stems respectively.

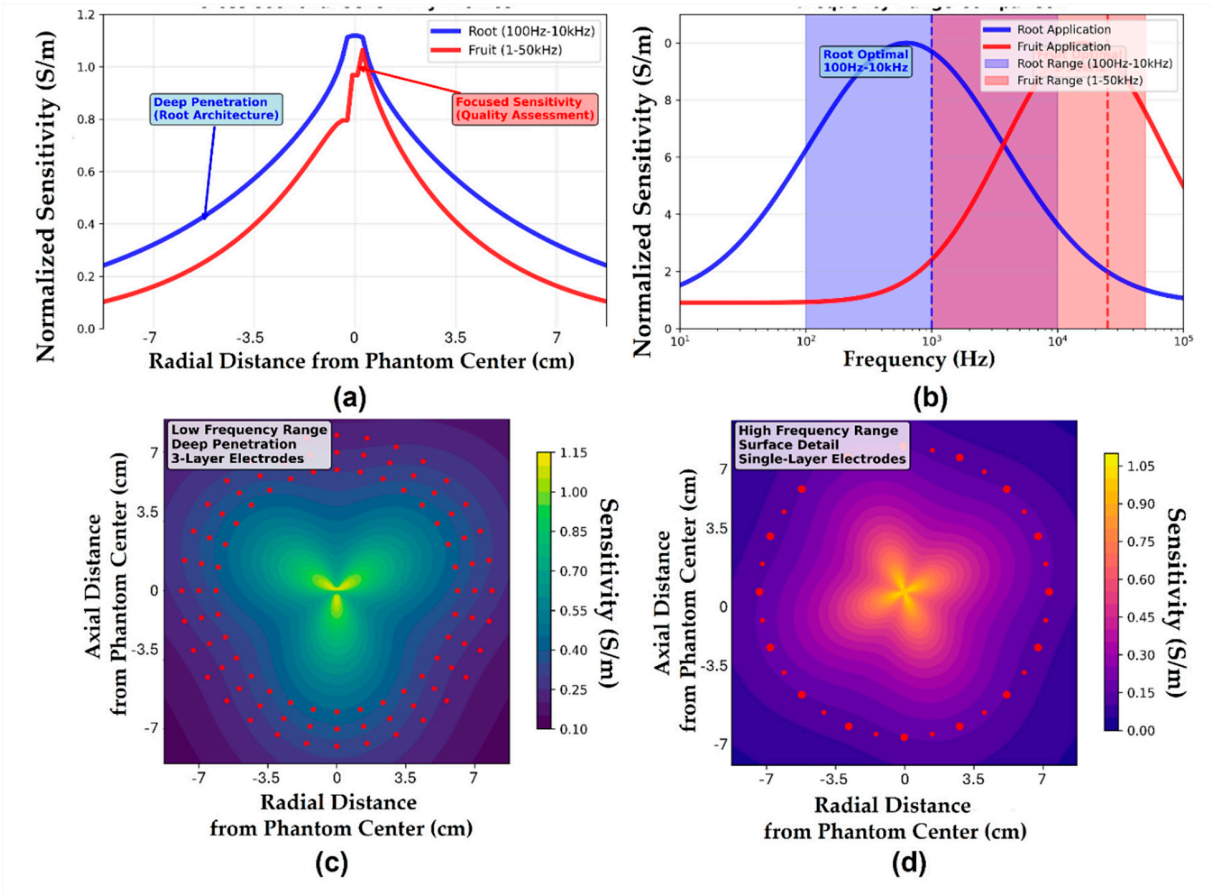
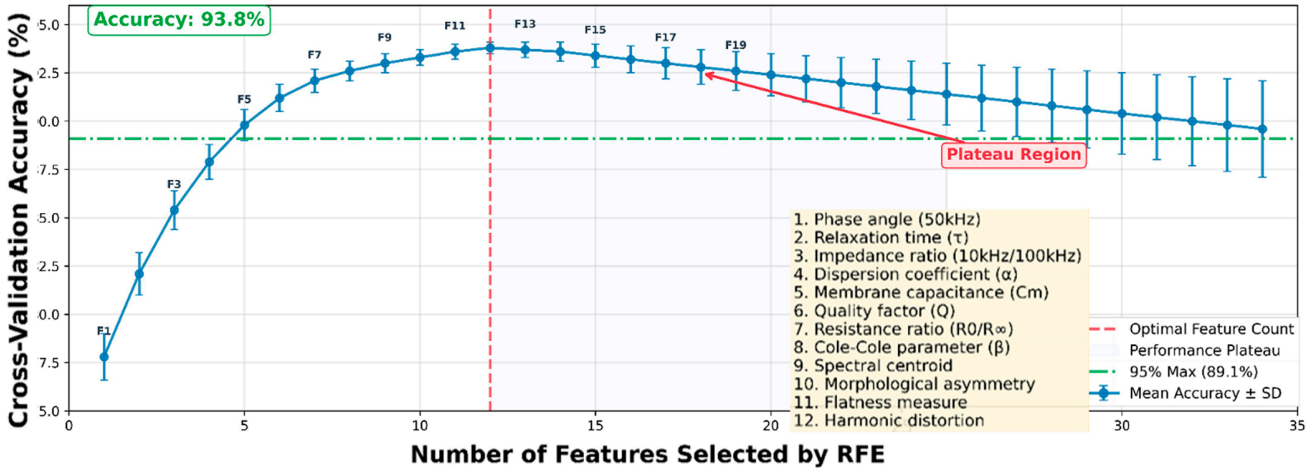
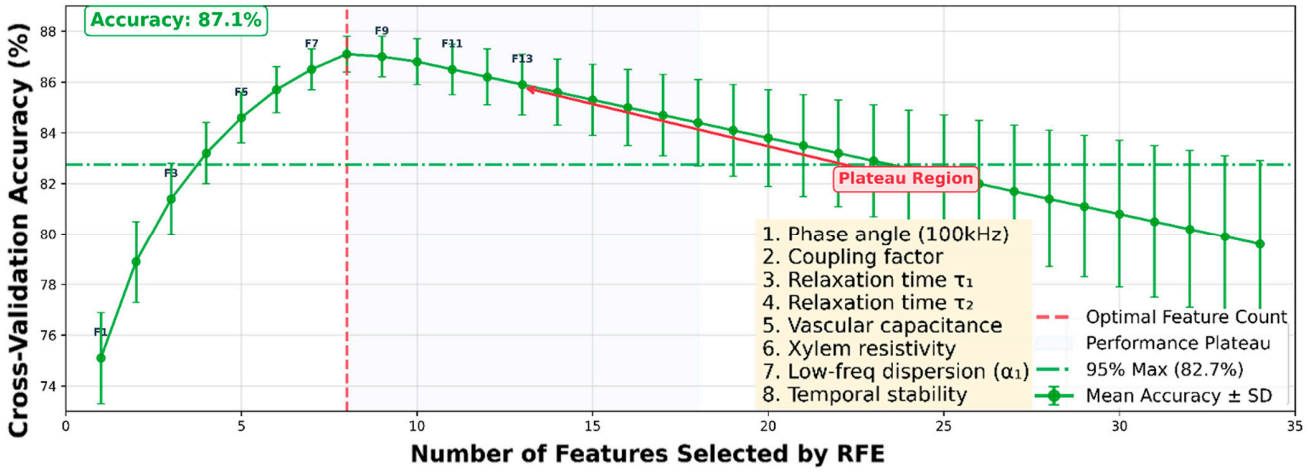


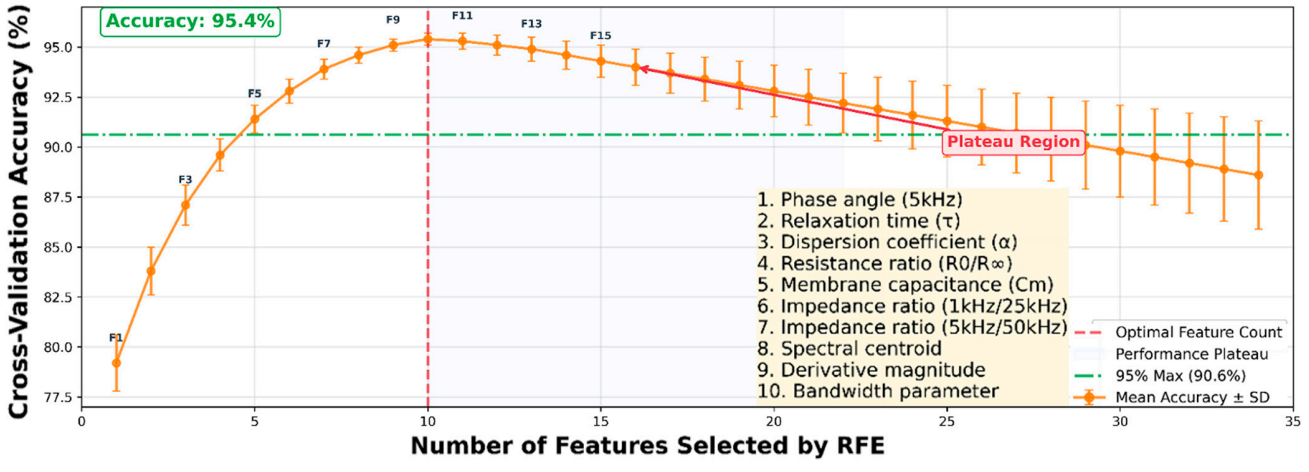
Figure S7. Frequency-dependent sensitivity and penetration analysis for tomographic applications showing (a) radial sensitivity profiles, (b) frequency response optimization, (c) 3-layer array root conductivity reconstruction, and (d) 2D fruit conductivity reconstruction.



(a)



(b)

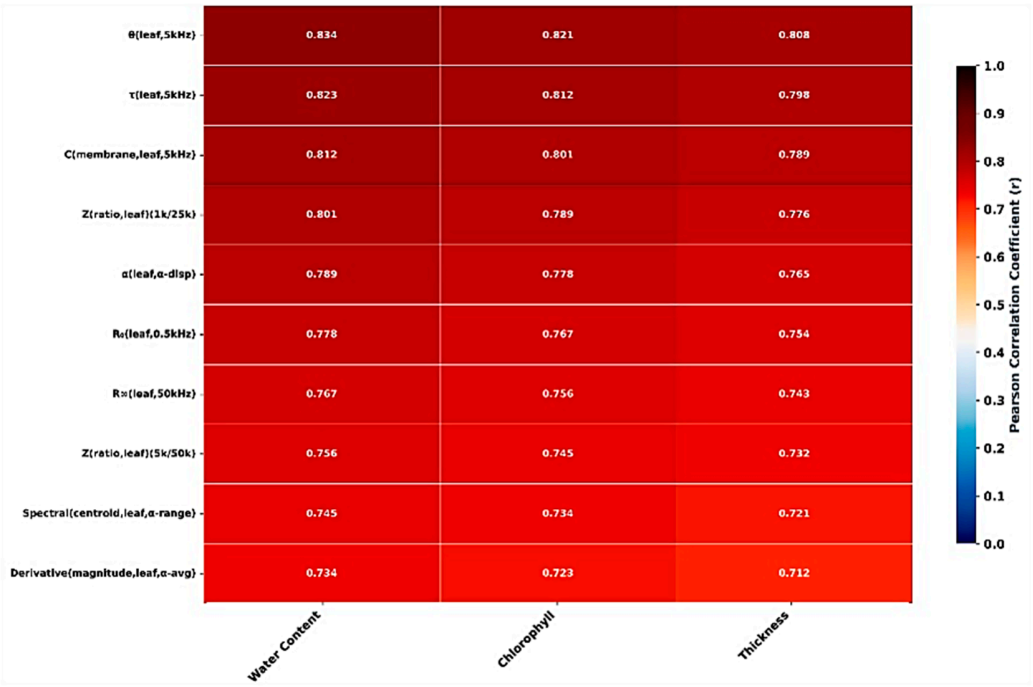


(c)

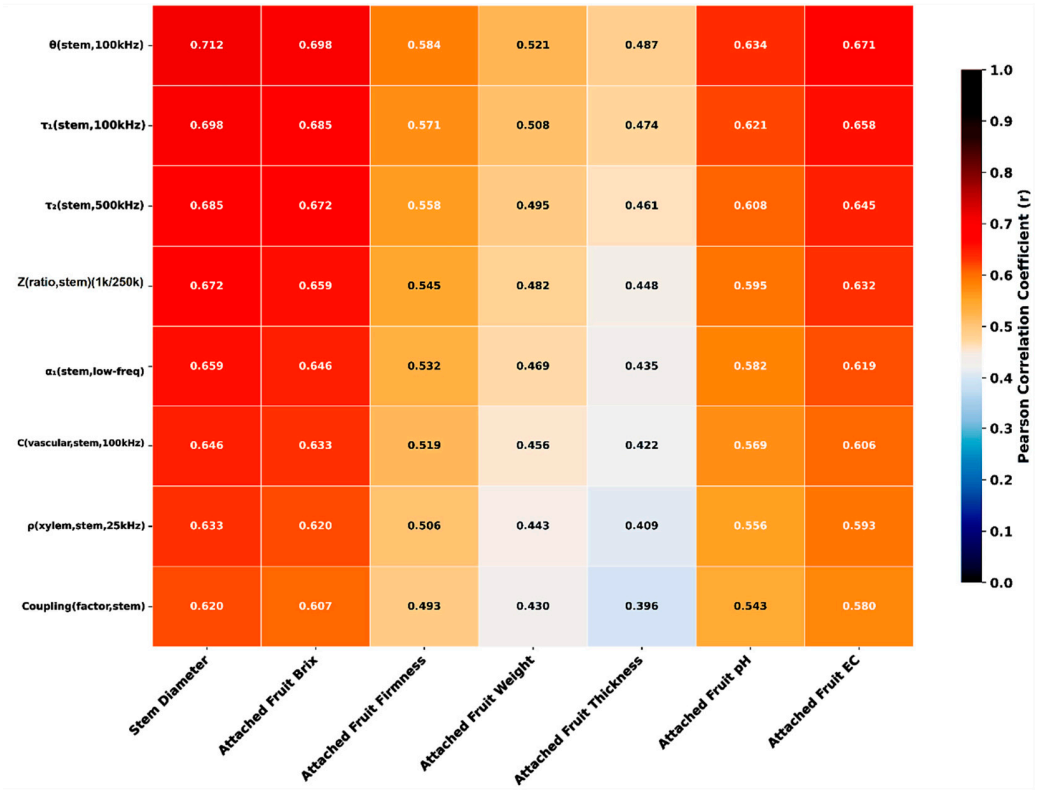
Figure S8. Recursive feature elimination with cross-validation (RFECV) results for optimal feature selection across (a) fruit maturity, (b) leaf water status, and (c) stem productivity classification tasks.


θ(fruit,50kHz)
τ(fruit,50kHz)
Q(factor,fruit,50kHz)
C(membrane,fruit,50kHz)
L(fruit,100kHz)
α(fruit,β-dlsp)
Rα(fruit,1kHz)
Z(ratio,fruit)(10k/100k)
Morphological(asymmetry,fruit)
Spectral(centroid,fruit,β-range)
R∞(fruit,200kHz)
Peak(power,fruit,50kHz)
0.923 0.912 0.687 0.654 0.843 0.896
0.908 0.894 0.672 0.641 0.829 0.881
0.896 0.887 0.698 0.665 0.856 0.874
0.887 0.878 0.681 0.648 0.834 0.869
0.874 0.865 0.663 0.631 0.821 0.856
0.869 0.858 0.656 0.624 0.812 0.847
0.856 0.847 0.649 0.617 0.798 0.834
0.863 0.852 0.671 0.639 0.805 0.841
0.847 0.836 0.692 0.659 0.789 0.823
0.834 0.823 0.678 0.645 0.776 0.812
0.821 0.812 0.665 0.632 0.763 0.798
0.812 0.801 0.658 0.625 0.754 0.789
Brix Content
Firmness
Weight
Thickness
Juice pH
Juice EC
Pearson Correlation Coefficient (r)
1.0
0.9
0.8
0.7
0.6
0.5
0.4
0.3
0.2
0.1
0.0

(a)


θ(leaf,5kHz)
τ(leaf,5kHz)
C(membrane,leaf,5kHz)
Z(ratio,leaf)(1k/25k)
α(leaf,α-dlsp)
Rα(leaf,0.5kHz)
R∞(leaf,50kHz)
Z(ratio,leaf)(5k/50k)
Spectral(centroid,leaf,α-range)
Derivative(magnitude,leaf,α-avg)
0.834 0.821 0.808
0.823 0.812 0.798
0.812 0.801 0.789
0.801 0.789 0.776
0.789 0.778 0.765
0.778 0.767 0.754
0.767 0.756 0.743
0.756 0.745 0.732
0.745 0.734 0.721
0.734 0.723 0.712
Water Content
Chlorophyll
Thickness
Pearson Correlation Coefficient (r)
1.0
0.9
0.8
0.7
0.6
0.5
0.4
0.3
0.2
0.1
0.0

(b)



(c)

Figure S9. Bioelectrical feature-validation metric correlation matrices for (a) fruits showing 12 features vs 6 established validation metrics, (b) leaves showing 10 features vs 3 metrics, and (c) stems showing 8 features vs 7 metric.